



TITLE:

Constitutive exposure of phosphatidylserine on viable cells.

AUTHOR(S):

Segawa, Katsumori; Suzuki, Jun; Nagata,
Shigekazu

CITATION:

Segawa, Katsumori ...[et al]. Constitutive exposure of phosphatidylserine on viable cells..
Proceedings of the National Academy of Sciences of the United States of America 2011,
108(48): 19246-19251

ISSUE DATE:

2011-11-29

URL:

<http://hdl.handle.net/2433/152171>

RIGHT:

©2012 by the National Academy of Sciences; この論文は出版社版であり
ません。引用の際には出版社版をご確認ご利用ください。; This is
not the published version. Please cite only the published version.

Classification: Biological Science, Cell Biology

Constitutive exposure of phosphatidylserine on viable cells

Katsumori Segawa^a, Jun Suzuki^a and Shigekazu Nagata^{a,b,1}.

^aDepartment of Medical Chemistry, Graduate School of Medicine, Kyoto University,
Yoshida-konoe, Kyoto 606-8501, Japan

^bCore Research for Evolutional Science and Technology, Japan Science and Technology
Corporation, Kyoto 606-8501, Japan

Key words: Phospholipid scramblase, apoptosis, macrophage, engulfment

¹Correspondence should be addressed to
Shigekazu Nagata,
Kyoto University Graduate School of Medicine,
Department of Medical Chemistry,
Yoshida-Konoe, Sakyo, Kyoto 606-8501, Japan
Tel: 81-75-753-9441, Fax: 81-75-753-9446,
E-mail: snagata@mfour.med.kyoto-u.ac.jp

Abstract

Apoptotic cells are quickly recognized and engulfed by phagocytes to prevent the release of noxious materials from dying cells. Phosphatidylserine (PS) exposed on the surface of apoptotic cells is a proposed ‘eat me’ signal for the phagocytes. TMEM16F, a membrane protein with 8 transmembrane segments, has the Ca-dependent phospholipid scramblase activity. Here we show that when lymphoma cells were transformed with a constitutively active form of TMEM16F, they exposed a high level of PS that was comparable to that observed on apoptotic cells. The PS-exposing cells were morphologically normal, and grew normally. They efficiently responded to interleukin 3, and underwent apoptosis upon treatment with Fas ligand. The viable PS-exposing cells bound to peritoneal macrophages at 4°C, but not at 25°C. Accordingly, these cells were not engulfed by macrophages. When apoptotic cells were injected i.v. into mice, they were phagocytosed by CD11c⁺CD8⁺ dendritic cells (DCs) in the spleen, but the PS-exposing living cells were not phagocytosed by these DCs. Furthermore, when PS-exposing lymphoma cells were transplanted s.c. into nude mice, they generated tumors as efficiently as parental lymphoma cells that did not expose PS. These results indicated that PS exposure alone is not sufficient to be recognized by macrophages as an “eat me” signal.

Introduction

Many harmful and unnecessary cells are generated during animal development, and they undergo apoptosis (1). In adults, senescent cells and virus- or bacteria-infected cells are removed by apoptosis (2). Apoptotic cells are swiftly engulfed by macrophages or immature dendritic cells to prevent the release of noxious materials from the dying cells that may activate the immune system, leading to the autoimmune disease (3, 4).

Macrophages specifically engulf apoptotic cells, but not living ones, indicating that the dying cells present an ‘eat me’ signal(s) to the phagocytes. Phosphatidylserine (PS), which is present on the inner leaflet of plasma membranes in healthy cells, is quickly exposed to the outer plasma membrane of apoptotic cells, and has been proposed as an ‘eat me’ signal (5). In fact, masking the PS on apoptotic cells inhibits their engulfment in vitro and in vivo (6, 7), strongly supporting the identification of PS as an ‘eat me’ signal.

The asymmetrical distribution of phospholipids on the plasma membrane is mediated by various transporters (8): ATP-dependent aminophospholipid translocase or flippase transports aminophospholipids from the outer leaflet to the cytoplasmic side. In addition, a Ca-dependent scramblase bidirectionally transports phospholipids. We recently identified TMEM16F (Transmembrane protein 16F), also called anoctamin 6, as this phospholipid scramblase (9). During that study, we noticed that an Asp-to-Gly point mutation at amino acid position 409 renders the molecule constitutively active; cells that express this mutant form of TMEM16F constitutively expose PS on their surface.

In this report, we found that there is an alternatively spliced variant of mouse TMEM16F. Mouse lymphoma cells expressing the TMEM16F splice variant with the Asp-to-Gly mutation exposed more PS than those expressing the authentic TMEM16F splice form with the same point mutation. These high-PS-exposing lymphoma cells grew normally, and responded normally to interleukin (IL) 3 by proliferating and to Fas ligand (FasL) by becoming apoptotic. The level of PS exposed on these cells was comparable to that observed on apoptotic cells. However, peritoneal macrophages did not engulf the viable PS-exposing cells, even though they efficiently engulfed apoptotic cells in a PS-dependent manner. When these living PS-exposing cells were transplanted into nude mice, they grew as aggressively as the parental lymphoma cells. These results indicate that although PS exposure is essential as an “eat me” signal, it is not sufficient for the apoptotic cells to be engulfed.

Results

PS exposure by TMEM16F mutants. We previously established a subline of Ba/F3 that strongly exposes PS in response to a Ca-ionophore (9). Expression cloning of the gene responsible for the PS exposure in this cell line identified a mutant TMEM16F that carried an Asp-to-Gly point mutation at codon 409 (D409G)(Fig. 1A). Further screening of the library led to the identification of the cDNA for a splice variant with the same point mutation generated by the insertion of an extra exon from intron 1 of the TMEM16F gene (Fig. 1B). The protein (D430G-long or D430G-L) which carried an extra peptide of 21 amino acids at amino acid position 24 (Fig. 1C), showed scramblase activity that was apparently stronger than that of the D409G. As shown in Fig. 1D, introduction of the wild-type TMEM16F into Ba/F3 did not confer the cells to expose PS. When the D409G mutant was expressed in Ba/F3, about 70% of the cells constitutively exposed PS. On the other hand, Ba/F3 cells expressing D430G-L exposed PS more strongly than those expressing D409G, indicating that the 21-amino acid insertion in the first cytoplasmic region of mouse TMEM16F has a positive effect on its scramblase activity. A similarly high level of PS exposure was observed when D430G-L was expressed in mouse WR19 cell transformants (W3-Ildm) expressing mouse Fas and the caspase-resistant form of ICAD (inhibitor of caspase-activated DNase) (10)(Fig. 1D).

Effect of constitutive PS exposure on cell growth and apoptosis. The asymmetrical

distribution of phospholipids on the inner and outer plasma membrane is thought to be important for maintaining the integrity of plasma membranes (8). However, the Ba/F3-D430G-L cells, which constitutively exposed PS, grew as efficiently as the parental Ba/F3 cells; the doubling time of both Ba/F3 and Ba/F3-D430G-L cells in the presence of 100 units/ml mouse IL-3 was 11.5 h (Fig. 2A). Accordingly, the dose-dependent response of the Ba/F3-D430G-L cells to IL-3 was comparable to that of the parental Ba/F3 cells (Fig. 2B). The expression of the TMEM16F mutant or constitutive exposure of PS also had no effect on the growth of W3-Ildm cells (Fig. 2C). That is, the parental W3-Ildm and their D430G-L transformants grew at a comparable rate (doubling time of 12.5 h). The W3-Ildm cells over-express Fas, and are sensitive to FasL-induced apoptosis (10, 11). The dose-dependent response to recombinant FasL was comparable between W3-Ildm and its transformants expressing D430G-L (Fig. 2D). These results suggested that the constitutive exposure of PS had little effect on the binding of IL-3 or FasL to its respective receptor, and that the signal transduction induced by IL-3 to promote cell growth or by FasL to promote apoptosis occurs normally.

Strong PS exposure on living cells. We then compared the level of PS exposed on the cell surface of the living W3-D430G-L cells with that on apoptotic cells. As shown in Fig. 3A, the Forward Scatter (FSC) and Side Scatter (SSC) profiles were similar between the W3-Ildm and W3-D430G-L cells. A small percentage of the W3-Ildm cells were

AnnexinV- and Sytox blue-positive, indicating that they underwent necrosis under normal growth conditions. Except for these necrotic cells, more than 90% of the W3-Ildm cells were Annexin V-negative. The W3-D430G-L cells also included a small percentage of necrotic cells, but nearly 95% of them were Annexin V-positive (Fig. 3A).

When cells undergo apoptosis, their size decreases and cellular granularity increases (12). Accordingly, when the W3-Ildm and W3-D430G-L cells were treated with FasL for 2 h, the FSC decreased from 118 to 68, and SSC increased from 66 to 127 in both cell lines (Fig. 3A), confirming that the constitutive PS exposure did not inhibit the FasL-induced apoptosis. The induction of apoptosis by FasL treatment caused PS to the cell surface of W3-Ildm without increasing the amount of Annexin V- and Sytox Blue-double positive necrotic cells. On the other hand, the treatment of W3-D430G-L with FasL did not increase the staining intensity of the Annexin V-binding, indicating that PS was exposed on the living W3-D430G-L cells to the same extent as on those undergoing apoptosis. MFG-E8 specifically recognizes PS, independent of Ca (13), and it bound to the W3-D430G-L cells about as well as to the apoptotic W3-Ildm cells, indicating that both populations exposed PS at comparable levels (Fig. 3B).

The PS exposure was then examined by confocal fluorescence microscopy. As shown in Fig. 3C, almost none of the living W3-Ildm cells were labeled much, if at all, by FITC-labeled MFG-E8. In contrast, the shrunken and rounded FasL-treated W3-Ildm cells uniformly bound MFG-E8. The lack of microvilli on the cell surface of the FasL-treated

cells confirmed that they had undergone apoptosis (14). The living non-apoptotic W3-D430G-L cells were also uniformly labeled with MFG-E8, but the cells were distorted, and their microvilli were visible (Fig. 3D). Treatment of the W3-D430G-L cells with FasL caused them to shrink and become rounded, accompanied by smoothing of the cell surface, but it did not enhance their ability to bind MFG-E8, confirming that the level of exposed PS did not differ between the living and apoptotic W3-D430G-L cells.

No engulfment of the PS-exposing living cells by macrophages. Cells expressing the caspase-resistant form of ICAD do not undergo apoptotic DNA fragmentation (10). When these cells are engulfed by macrophages, DNase II in the lysosomes of the macrophages cleaves the DNA of the apoptotic cells. Using this system, we could distinguish the cells inside macrophages from those bound to the macrophage surface, to assay the engulfment of apoptotic cells (13). When FasL-treated W3-Ildm cells were co-incubated with thioglycollate-elicited peritoneal macrophages, 35-38% of the macrophages were stained with TUNEL (Fig. 4A). Microscopic observation of the macrophages confirmed that the apoptotic TUNEL-positive cells were inside the macrophages (Fig. 4B). The engulfment of the apoptotic W3-Ildm cells was PS-dependent, because it could be inhibited in a dose-dependent manner by the D89E mutant of MFG-E8 (Fig. 4C), which masks PS (13). On the other hand, like living W3-Ildm cells that did not expose PS, the PS-exposing living W3-D430G-L cells were not engulfed by the macrophages, although the cells could be

engulfed after they were treated with FasL (Fig. 4A and B).

Mouse resident peritoneal macrophages express Tim-4, which specifically binds PS (15). To examine whether the PS exposed on W3-D430G-L cells was sufficient for the cells to bind macrophages, the cells were labeled with the cell-tracker CMRA, and incubated with macrophages. As shown in Fig. 4D and E, when the co-incubation was performed at 4°C, the apoptotic W3-Ildm cells and the living W3-D430G-L cells, but not the living W3-Ildm cells, slowly bound to the macrophages. On the other hand, when the incubation temperature was increased to 25°C, the apoptotic W3-Ildm and apoptotic W3-D430G-L cells quickly bound to the macrophages, but the ability of the living W3-D430G-L cells to bind the macrophages was lost. These results suggested that the affinity of PS-exposing living W3-D430G-L cells for macrophages is weaker than that of apoptotic cells.

No clearance of phosphatidylserine-exposing cells in vivo. Circulating apoptotic cells are engulfed in the spleen by CD8 α ⁺CD11c⁺ dendritic cells (DCs) in a PS-dependent manner (16, 17). To investigate whether the viable PS-exposing cells could be engulfed by DCs, the CMRA-labeled viable or apoptotic W3-Ildm and W3-D430G-L cells were injected into syngeneic BALB/c mice. As shown in Fig. 5A, about 20% of the CD8 α ⁺ DCs in the spleen carried apoptotic cells 30 min after the administration of dead cells. On the other hand, when the living W3-Ildm cells were injected, 6-8% of the CD8 α ⁺ DCs were CMRA-positive, suggesting that some population of W3-Ildm cells underwent apoptosis in

vivo. The percentage of CMRA-positive $CD8\alpha^+$ DCs obtained with the PS-exposing living W3-D430G-L cells was comparable to that obtained with the living W3-Ildm cells, indicating that the exposed PS was not sufficient for the viable cells to be engulfed by splenic $CD8\alpha^+$ DCs.

To confirm that the PS-exposing cells were not recognized by phagocytes in vivo, the W3-Ildm and W3-D430G-L cells were injected into BALB/c nude mice. As shown in Fig. 5B, both the W3-Ildm and W3-D430G-L cells generated tumors, which were of comparable size on day 28. Flow cytometry analysis of the recovered day 28-tumor cells revealed that a significant population (about 33%) of W3-D430G-L but not W3-Ildm cells constitutively exposed PS (Fig. 5C). The apparent reduction of the PS-exposing cells could be due to the poor environmental conditions (hypoxia and acidic conditions) for the tumor cells.

Discussion

In this report, we found that the insertion of a 21-amino acid peptide at the N-terminal cytoplasmic region of TMEM16F strengthened the scramblase activity of its constitutively active mutant. Treating the cells with a Ca-chelator blocked the PS exposure caused by the mutant, suggesting that the mutant still required Ca for the scrambling activity. We used these high-PS-exposing cells to study the effects of cell-surface PS on cell growth and recognition by macrophages.

We found that mouse lymphoma cells exposing a high level of PS could efficiently respond to cytokines, and grew normally *in vitro* and *in vivo*. In cells expressing the D409G mutant of TMEM16F, not only PS, but also phosphatidylethanolamine is exposed, and phosphatidylcholine and sphingomyelin are constitutively internalized (9), suggesting that the asymmetrical distribution of phospholipids is largely disrupted in these cells. When IL-3 and FasL bind to their receptors, the resulting ligand/receptor complexes are internalized through the lipid raft/caveolar pathway for signal transduction (18, 19). Lipid rafts are heterogeneous domains of cell membranes that are rich in cholesterol, glycosphingolipids and phospholipids, and lipids play an essential role in maintaining the integrity of rafts (20). In this regard, it was very surprising to find that the PS-exposing cells responded to IL-3 and FasL as efficiently as the PS-non-exposing parental cells. It will be interesting to examine whether lipid rafts are present in the PS-exposing cells, and how the IL-3-IL-3-receptor complex and FasL-Fas complex are internalized for the signal

transduction in these cells.

PS is exposed during apoptotic cell death, and its exposure is necessary for the dead cells to be engulfed by macrophages (4, 21). PS is exposed in other situations, too. For example, activated platelets, mast cells, and neutrophils expose PS (22), while myocytes and trophoblasts transiently expose PS during their maturation (23, 24). Annexin V can bind to activated lymphocytes under some conditions (25-28), and to an ovarian carcinoma cell line (29), suggesting that these cells may also expose PS. Except for the activated neutrophils, these PS-exposing cells are not engulfed by macrophages. On the other hand, Fadok et al. reported that when the outer leaflets of living cells are enriched with PS by liposomes, the living cells are engulfed by macrophages (5). In contrast, we found that mouse lymphoma cells exposing PS were not engulfed if they were alive. This may agree with the previous report that the PS-exposure alone on apoptotic cells is insufficient to be recognized by human monocytes-derived macrophages (30). Borisenko et al (31) proposed that macrophages have a sensitivity threshold for the externalized PS for engulfment. However, the level of PS exposed on the surface of the viable W3-D430G-L was comparable to that observed on apoptotic cells, yet the former were not engulfed by macrophages, indicating that the PS level was not critical for determining whether the cells are engulfed or not.

We found that the living PS-exposing cells bound to Tim-4-expressing resident peritoneal macrophages at 4°C, but not at 25°C, whereas the apoptotic cells quickly and

tightly bound the same macrophages at 25°C. These results suggest that PS exposed on the living cells is qualitatively different from the PS on apoptotic cells. Human Jurkat cells undergoing apoptosis expose oxidized PS (32), and MFG-E8, an opsonin for apoptotic cell engulfment, binds to oxidized PS with higher affinity than to non-oxidized PS (33). It will be interesting to examine whether or not the oxidization of PS exposed on viable cells allows them to be phagocytosed by macrophages.

Other possible differences between viable and apoptotic PS-exposing cells are that viable cells present “don’t eat me” signal(s) or apoptotic cells expose additional “eat me” signal(s) (3). Various molecules such as CD47, CD31, and PAI-1 (34-37) have been proposed as “don’t eat me” signals. The PS-exposing W3-D430G-L cells do not express CD47, and antibodies against CD47 or its receptor SHPS-1 did not promote the engulfment of living W3-D430G-L cells by macrophages, indicating that CD47 is not responsible for preventing the engulfment, at least in this system. Regarding additional “eat me” signals, Gardai et al (38) reported that calreticulin is exposed on apoptotic cells, and promotes their engulfment. However, bovine calreticulin had no effect on the engulfment of W3-D430G-L cells by macrophages.

In conclusion, we showed here that PS exposed on apoptotic cells is required but not sufficient for the dead cells to be engulfed. Another mechanism(s), a modification of PS, or additional molecules that could be “don’t eat me” or “eat me” signal(s), must be involved for the efficient engulfment of apoptotic cells. The cell line established in this report, which

strongly exposes PS while remaining viable, will be useful for elucidating how macrophages recognize apoptotic cells for engulfment.

Materials and Methods

Mice, cell lines, recombinant proteins, and reagents. C57BL/6J, BALB/c, and BALB/c nude mice were purchased from Clea Japan. All mouse studies were approved by the Ethics Review Committee for Animal Experimentation of the Graduate School of Medicine, Kyoto University. Mouse IL-3-dependent Ba/F3 cells were maintained in RPMI medium containing 10% fetal calf serum (FCS; Gibco), 100 U/ml mouse IL-3 and 50 μ M 2-mercaptoethanol. W3-Ildm is a transformant of mouse T-cell lymphoma (WR19L) that expresses mouse Fas and a caspase-resistant form of the inhibitor of caspase-activated DNase (ICAD) (10), and was cultured in DMEM containing 10% FCS. Mouse IL-3 was produced by mouse C127I cells transformed with a bovine papillomavirus expression vector bearing IL-3 cDNA as described (39). The biological activity of the mouse IL-3 was determined with Ba/F3 cells, and one unit is defined as the dilution that gives a half-maximum response. The recombinant soluble form of human Fas ligand (FasL) and the D89E mutant of mouse MFG-E8 were produced in COS7 and HEK293T cells respectively, and purified as described (13, 40). The biological activity of FasL was determined with W3-Ildm cells, and one unit is defined as that dilution that gives a half-maximum response. The FITC-labeled bovine MFG-E8 (BLAC-FITC) was from Hematologic Technologies. CellTrackerTM Orange CMRA was from Invitrogen. Rat mAbs against mouse Mac-1 (clone M1/70), Fc γ RII/III (clone 2.4G2), CD11c (clone HL3), Thy1.2 (clone 53-2.1), and CD8 α (clone 53-6.7) were purchased from BD Pharmingen.

Transformation of mouse Ba/F3 and W3-Ildm cells. Ba/F3 and W3-Ildm cells were subjected to ecotropic and amphotropic retrovirus-mediated transformation, respectively. In brief, the retrovirus carrying the Flag-tagged TMEM16F cDNA was produced by introducing the pMX-puro vector into Plat-E cells expressing MuLV gag-pol and env (41), or into 293T cells with the amphotrophic retrovirus-packaging construct pE-Ampho (Takara Bio). The retroviruses were concentrated by centrifugation at 6,000 x g for 16 h at 4°C, and used to infect Ba/F3 and W3-Ildm cells. The transformants were selected by culturing the cells in the presence of 1 µg/ml puromycin. If necessary, a population (1-5%) of the transformants that was strongly stained with Annexin V was sorted by FACS Aria (BD Bioscience) for further studies.

Induction of apoptosis, and detection of phosphatidylserine. To induce apoptosis, cells (1.0×10^6 cell/ml) were incubated with 100 U/ml FasL at 37°C for 2 h. The cell viability was assayed by WST-1 assay with 2-(4-Iodophenyl)-3-(4-nitrophenyl)-5-(2,4-disulfophenyl)-2H-tetrazolium, monosodium salt (WST-1; Dojin Laboratories) and 1-Methoxy-5-methylphenazinium methylsulfate as described (11). To detect PS, cells were stained at 25°C for 5 min with 1,000-2,000-fold diluted Cy5-labeled Annexin V (Biovision) or 800 ng/ml FITC-MFG-E8 in staining buffer [10 mM Hepes-KOH (pH 7.4) containing 140 mM NaCl and 2.5 mM CaCl_2], followed by

incubation with 500 nM SYTOX Blue, and analyzed by FACS Aria. For microscopic observation, 2×10^5 cells in 8-well Lab-Tek II chamber slides (Nalge Nunc) were incubated on ice for 15 min with 4 μ g/ml FITC-MFG-E8 in staining buffer, and observed by fluorescence microscopy (FV1000-D, Olympus).

Preparation of macrophages, and in vitro phagocytosis assay. Resident peritoneal macrophages were prepared from 6-12-week old C57BL/6J mice as described (15). To prepare thioglycollate-elicited peritoneal macrophages, the mice were injected with 60 mg of thioglycollate, and the peritoneal macrophages were collected 4 days later. The in vitro phagocytosis assay was performed as described previously (13, 42). In brief, 6×10^5 thioglycollate-elicited peritoneal macrophages were grown overnight in 12-well cell culture plates (Corning). Apoptotic or PS-exposing cells (3×10^6) were added to the macrophages, and the mixture was incubated at 37°C for 2 h in the presence of 1 μ g/ml rat anti-mouse Fc γ RII/III. Macrophages were detached from the plate by treatment with 0.25% trypsin in PBS containing 1 mM EDTA, and stained with APC-conjugated rat anti-mouse Mac-1, followed by TUNEL staining with FITC-labeled dUTP (Roche Molecular Biochemicals). Flow cytometry was conducted using a FACS Aria, and the percentage of phagocytosis was defined as the percentage of TUNEL-positive cells in the Mac-1-positive population. In some cases, peritoneal macrophages (6×10^4 cells) were incubated with living or apoptotic cells (3×10^5 cells/well) in 8-well Lab-Tek II chambers. After fixation with 1%

paraformaldehyde, the cells were subjected to TUNEL staining using the Apoptag kit (Millipore), and observed by fluorescence microscopy.

Binding of PS-exposing cells to macrophages. CMRA-labeled living or apoptotic cells ($2.5\text{--}5 \times 10^5$ cells) were co-incubated in suspension with freshly prepared peritoneal cells (1×10^5 cells) in PBS supplemented with 10% FCS. The cells were stained with APC-conjugated anti-Mac-1, followed by 500 nM SYTOX Blue, and analyzed by FACS Aria. For microscopic observation, 1×10^5 peritoneal cells were seeded into 8 -well Lab-Tek II chambers, incubated at 37°C for 2 h, and washed with PBS containing 10% FCS. CMRA-labeled cells (5×10^5 cells) were added to the well, and the mixture was incubated on ice for 1 h. After the incubation, cells were washed three times with pre-chilled PBS, stained with Alexa fluor 488-conjugated anti-Mac-1 for 5 min on ice, and observed by fluorescence microscopy (BioRevo BZ-9000, Keyence).

In vivo phagocytosis assay, and tumor development. The in vivo phagocytosis assay was carried out as described (17). In brief, 5×10^7 W3-Ildm living cells were pre-incubated for 60 min with a caspase inhibitor, 10 μ M Q-VD-OPh (R&D systems), and stained at 25°C for 30 min with 4 μ M 5-(((4-chloromethyl)benzoyl)amino) tetramethylrhodamine (CMRA) (Invitrogen). Apoptosis was induced by treating the cells with 100 U/ml FasL for 90 min at 37°C. Then, 3×10^7 CMRA-labeled cells in 300 μ l of PBS were injected i.v. into

8-weeks-old female BALB/c mice. Thirty minutes later, the spleens were dissected, flushed with 100 U/ml collagenase D (Roche Diagnosis), teased apart with fine forceps, and digested with 400 U/ml collagenase D for 30 min at 37°C. After hemolysis with EL buffer (Qiagen), the DCs were enriched by MACS sorting with anti-mouse CD11c microbeads (Miltenyi Biotec). They were then stained with APC- rat anti-mouse CD11c and FITC- rat anti-mouse CD8 α , followed by staining with 500 nM SYTOX Blue, and analyzed by FACS Aria. In some cases, the CMRA-positive cells in the CD11c⁺CD8 α ⁺ population were sorted by FACS Aria, and observed by fluorescence microscopy.

To examine the ability of lymphoma to grow in vivo, cells (1×10^6) were injected into 8-week-old female BALB/c nude mice. Four weeks later, the tumors were dissected, and their weight was determined. The dissected tumors were further teased apart with fine forceps, and digested with collagenase D as described above. After passing through mesh, the cells were washed with cold PBS, and stained with Cy5-labeled Annexin V, followed by staining with 1 μ g/ml FITC-rat anti- mouse Thy1.2 and SYTOX Blue, and analyzed by FACS Aria.

Statistical analysis. All data were expressed as the mean with SD. Differences between groups were examined for statistical significance using the Student's *t*-test with the Bonferroni correction.

Conflict of interest

The authors declare no conflict of interest.

ACKNOWLEDGEMENTS. We thank M. Fujii and M. Harayama for secretarial assistance. This work was supported in part by Grants-in-Aid from the Ministry of Education, Science, Sports, and Culture in Japan. K.S. is a Research Fellow of the Japan Society for the Promotion of Science.

References

1. Jacobson MD, Weil M, Raff MC (1997) Programmed cell death in animal development. *Cell* 88:347-354.
2. Nagata S (1997) Apoptosis by death factor. *Cell* 88:355-365.
3. Ravichandran KS (2010) Find-me and eat-me signals in apoptotic cell clearance: progress and conundrums. *J Exp Med* 207:1807.
4. Nagata S, Hanayama R, Kawane K (2010) Autoimmunity and the clearance of dead cells. *Cell* 140:619-630.
5. Fadok VA, de Cathelineau A, Daleke DL, Henson PM, Bratton DL (2001) Loss of phospholipid asymmetry and surface exposure of phosphatidylserine is required for phagocytosis of apoptotic cells by macrophages and fibroblasts. *J Biol Chem* 276:1071-1077.
6. Krahling S, Callahan MK, Williamson P, Schlegel RA (1999) Exposure of phosphatidylserine is a general feature in the phagocytosis of apoptotic lymphocytes by macrophages. *Cell Death Differ* 6:183-189.
7. Asano K, *et al.* (2004) Masking of phosphatidylserine inhibits apoptotic cell engulfment and induces autoantibody production in mice. *J Exp Med* 200:459-467.
8. Balasubramanian K, Schroit A (2003) Aminophospholipid asymmetry: A matter of life and death. *Annu Rev Physiol* 65:701-734.

9. Suzuki J, Umeda M, Sims PJ, Nagata S (2010) Calcium-dependent phospholipid scrambling by TMEM16F. *Nature* 468:834-838.
10. Sakahira H, Enari M, Nagata S (1998) Cleavage of CAD inhibitor in CAD activation and DNA degradation during apoptosis. *Nature* 391:96-99.
11. Tanaka M, Suda T, Takahashi T, Nagata S (1995) Expression of the functional soluble form of human Fas ligand in activated lymphocytes. *EMBO J* 14:1129-1135.
12. Dive C, *et al.* (1992) Analysis and discrimination of necrosis and apoptosis (programmed cell death) by multiparameter flow cytometry. *Biochim Biophys Acta* 1133:275-285.
13. Hanayama R, *et al.* (2002) Identification of a factor that links apoptotic cells to phagocytes. *Nature* 417:182-187.
14. Morris R, Hargreaves A, Duvall E, Wyllie A (1984) Hormone-induced cell death. 2. Surface changes in thymocytes undergoing apoptosis. *Am J Pathol* 115:426-436.
15. Miyanishi M, *et al.* (2007) Identification of Tim4 as a phosphatidylserine receptor. *Nature* 450:435-439.
16. Iyoda T, *et al.* (2002) The CD8⁺ dendritic cell subset selectively endocytoses dying cells in culture and in vivo. *J Exp Med* 195:1289-1302.
17. Miyake Y, *et al.* (2007) Critical role of macrophages in the marginal zone in

- the suppression of immune responses to apoptotic cell-associated antigens. *J Clin Invest* 117:2268-2278.
18. Lei JT, Martinez-Moczygemba M (2008) Separate endocytic pathways regulate IL-5 receptor internalization and signaling. *J Leukoc Biol* 84:499-509.
 19. Grassme H, *et al.* (2001) CD95 signaling via ceramide-rich membrane rafts. *J Biol Chem* 276:20589-20596.
 20. Cheng ZJ, *et al.* (2006) Distinct mechanisms of clathrin-independent endocytosis have unique sphingolipid requirements. *Mol Biol Cell* 17:3197-3210.
 21. Erwig LP, Henson PM (2008) Clearance of apoptotic cells by phagocytes. *Cell Death Differ* 15:243-250.
 22. Lentz B (2003) Exposure of platelet membrane phosphatidylserine regulates blood coagulation. *Prog Lipid Res* 42:423-438.
 23. van den Eijnde S, *et al.* (2001) Transient expression of phosphatidylserine at cell-cell contact areas is required for myotube formation. *J Cell Sci* 114:3631-3642.
 24. Huppertz B, Bartz C, Kokozidou M (2006) Trophoblast fusion: fusogenic proteins, syncytins and ADAMs, and other prerequisites for syncytial fusion. *Micron* 37:509-517.

25. Fischer K, *et al.* (2006) Antigen recognition induces phosphatidylserine exposure on the cell surface of human CD8+ T cells. *Blood* 108:4094-4101.
26. Dillon SR, Mancini M, Rosen A, Schlissel MS (2000) Annexin V binds to viable B cells and colocalizes with a marker of lipid rafts upon B cell receptor activation. *J Immunol* 164:1322-1332.
27. Smrz D, Draberova L, Draber P (2007) Non-apoptotic phosphatidylserine externalization induced by engagement of glycosylphosphatidylinositol-anchored proteins. *J Biol Chem* 282:10487-10497.
28. Dias-Baruffi M, *et al.* (2003) Dimeric galectin-1 induces surface exposure of phosphatidylserine and phagocytic recognition of leukocytes without inducing apoptosis. *J Biol Chem* 278:41282-41293.
29. Rao LV, Tait JF, Hoang AD (1992) Binding of annexin V to a human ovarian carcinoma cell line (OC-2008). Contrasting effects on cell surface factor VIIa/tissue factor activity and prothrombinase activity. *Thromb Res* 67:517-531.
30. Devitt A, Pierce S, Oldreive C, Shingler W, Gregory C (2003) CD14-dependent clearance of apoptotic cells by human macrophages: the role of phosphatidylserine. *Cell Death Differ* 10:371-382.
31. Borisenko G, *et al.* (2003) Macrophage recognition of externalized

- phosphatidylserine and phagocytosis of apoptotic Jurkat cells--existence of a threshold. *Arch Biochem Biophys* 413:41-52.
32. Tyurina YY, *et al.* (2004) Lipid antioxidant, etoposide, inhibits phosphatidylserine externalization and macrophage clearance of apoptotic cells by preventing phosphatidylserine oxidation. *J Biol Chem* 279:6056-6064.
33. Borisenko GG, Iverson SL, Ahlberg S, Kagan VE, Fadeel B (2004) Milk fat globule epidermal growth factor 8 (MFG-E8) binds to oxidized phosphatidylserine: implications for macrophage clearance of apoptotic cells. *Cell Death Differ* 11:943-945.
34. Brown S, *et al.* (2002) Apoptosis disables CD31-mediated cell detachment from phagocytes promoting binding and engulfment. *Nature* 418:200-203.
35. Park YJ, *et al.* (2008) PAI-1 inhibits neutrophil efferocytosis. *Proc Natl Acad Sci USA* 105:11784-11789.
36. Nilsson A, Oldenborg PA (2009) CD47 promotes both phosphatidylserine-independent and phosphatidylserine-dependent phagocytosis of apoptotic murine thymocytes by non-activated macrophages. *Biochem Biophys Res Commun* 387:58-63.
37. Oldenborg PA, *et al.* (2000) Role of CD47 as a marker of self on red blood cells. *Science* 288:2051-2054.

38. Gardai SJ, *et al.* (2005) Cell-surface calreticulin initiates clearance of viable or apoptotic cells through trans-activation of LRP on the phagocyte. *Cell* 123:321-334.
39. Fukunaga R, Ishizaka-Ikeda E, Nagata S (1990) Purification and characterization of the receptor for murine granulocyte colony-stimulating factor. *J Biol Chem* 265:14008-14015.
40. Shiraishi T, *et al.* (2004) Increased cytotoxicity of soluble Fas ligand by fusing isoleucine zipper motif. *Biochem Biophys Res Commun* 322:197-202.
41. Kitamura T, *et al.* (2003) Retrovirus-mediated gene transfer and expression cloning: powerful tools in functional genomics. *Exp Hematol* 31:1007-1014.
42. Tada K, *et al.* (2003) Tethering of apoptotic cells to phagocytes through binding of CD47 to Src homology 2 domain-bearing protein tyrosine phosphatase substrate-1. *J Immunol* 171:5718-5726.

Legends to Figures

Fig. 1. Constitutive exposure of phosphatidylserine on TMEM16F mutants. (A) Schematic diagrams of mouse TMEM16F (wild-type) and its mutants D409G and D430G-L. The wild-type mouse TMEM16F is comprised of 911 amino acids. The D409 mutant carries a glycine residue in place of an aspartic acid at codon 409. In the D430G-L mutant, a 21-amino acid peptide is inserted at amino acid position 24. (B) A splice variant produces TMEM16F carrying an extra peptide. A population of TMEM16F mRNA uses a sequence in intron 1 as an extra exon that codes for 21 amino acids. (C) Schematic representation of TMEM16F mutants. The Asp-to-Gly point mutation is in the first cytoplasmic loop, while the 21-amino acid insertion is in the N-terminal cytoplasmic domain. (D) Left four panels, Ba/F3 cells were transformed with the empty vector, wild-type TMEM16F, its D409G mutant, or its D430G-L mutant. The amount of PS exposed on the cells was analyzed by Cy5-labeled Annexin V, followed by FACS analysis. In the right panel, W3-Ildm cells were transformed with D430G-L, and the PS exposure was analyzed as above.

Fig. 2. No effect of phosphatidylserine exposure on cell growth or cytokine responses. (A) Mouse Ba/F3 and Ba/F3-D430G-L cells were seeded at 10^4 cells/ml in 1 ml of RPMI1640 medium containing 10% FCS and 100 units/ml mouse IL-3, and cultured at 37°C for 6 days. The cells were split 1:100 every 3 days, and their growth was followed. (B) Ba/F3 and Ba/F3-D430G-L cells were washed with RPMI1640 containing 10% FCS, and cultured at

37°C for 48 h in medium containing the indicated concentration of mouse IL-3. The cell viability was then determined by the WST-1 assay, and is expressed as the percentage of that obtained with 64 units/ml IL-3. (C) Mouse W3-Ildm and W3-D430G-L cells were seeded at 3×10^4 cells/ml in 1 ml of RPMI1640 medium containing 10% FCS, and cultured at 37°C for 9 days. The cells were split 1:80 every 3 days, and the cell growth was followed. (D) W3-Ildm and W3-D430G-L cells were incubated at 37°C for 4 h with the indicated concentration of human FasL. The cell viability was then determined by the WST-1 assay, and is expressed as the percentage of that without FasL.

Fig. 3. Exposure of phosphatidylserine on living W3-D430G-L cells. (A) W3-Ildm and W3-D430G-L cells with or without FasL treatment were stained with Cy5-labeled Annexin V and SytoxBlue, and analyzed by flow cytometry. The left 4 panels show the FSC-SSC profile, while the right 4 panels show the profile for Annexin V-SytoxBlue staining. (B) W3-Ildm and W3-D430G-L cells with or without FasL treatment were stained with the FITC-labeled MFG-E8, and analyzed by FACS. The MFG-E8 staining profile in the Sytox Blue-negative population is shown. (C and D) W3-Ildm and W3-D430G-L cells with or without FasL treatment were stained with FITC-labeled MFG-E8, and observed by confocal fluorescence microscopy. Images for MFG-E8 (green) and differential interference contrast (DIC) are shown. Arrowheads indicate microvilli. Scale bar, 10 μ m.

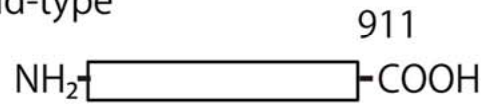
Fig. 4. No engulfment of the PS-exposing living cells by macrophages. (A) TUNEL staining profile of Mac-1⁺ thioglycollate-elicited peritoneal macrophages. W3-Ildm and W3-D430G-L cells that had been untreated or treated with FasL were co-incubated for 2 h, subjected to TUNEL-staining, and analyzed by FACS. The TUNEL staining profile of the Mac-1⁺ population is shown. The number indicates the percentage of TUNEL-positive cells. (B) W3-Ildm and W3-D430G-L cells that had been untreated or treated with FasL were co-incubated for 2 h with thioglycollate-elicited peritoneal macrophages, stained for TUNEL and DAPI, and observed by confocal microscopy. Images for TUNEL (green) and merged images for TUNEL, DAPI, and DIC are shown. Scale bar, 10 μ m. (C) W3-Ildm cells were treated with FasL, incubated at 25°C for 5 min with the indicated concentrations of the D89E mutant of mouse MFG-E8, and co-incubated for 2 h with thioglycollate-elicited peritoneal macrophages. The macrophages were then subjected to TUNEL staining, followed by flow cytometry. The phagocytosis index indicates the percentage of TUNEL-positive macrophages. (D) Binding of the PS-exposing cells to macrophages. Untreated or FasL-treated CMRA-labeled W3-Ildm and W3-D430G-L cells (5×10^5 cells for 4°C, and 2.5×10^5 cells for 25°C incubation) were incubated at 4°C or 25°C for the indicated period with resident peritoneal cells (1×10^5 cells). The cells were stained with APC-labeled anti-Mac-1, and analyzed by flow cytometry. The percentage of CMRA-positive macrophages in the Mac-1⁺ population is plotted. In left panels, representative FACS profiles in which the FasL-treated W3-Ildm cells were incubated at

25°C for 0 or 60 min are shown. (E) The CMRA-labeled W3-Ildm and W3-D430G-L (red) cells, with or without FasL-treatment, were incubated at 4°C for 60 min with resident peritoneal cells. They were thoroughly washed with cold PBS, stained with Alexa Fluor 488-anti-Mac1 (green), and observed by fluorescence microscopy. Arrows indicate macrophages surrounded by CMRA-labeled cells. Scale bar, 20 μ m.

Fig. 5. No clearance of the viable PS-exposing cells in vivo. (A) CMRA-labeled W3-Ildm and W3-D430G-L and FasL-treated W3-Ildm cells were injected into syngeneic female BALB/c mice. Thirty minutes after the injection, the splenic DCs were enriched by MACS sorting and analyzed by flow cytometry. The CMRA profile of the CD11c⁺CD8 α ⁺ population is shown. The Number indicates the percentage of CMRA-positive cells in the CD11c⁺CD8 α ⁺ population. Average values of 3-4 mice/group are shown with S.D. * $P < 0.01$. (B) Tumor development. W3-Ildm and W3-D430G-L cells (1.0×10^6 cells) were transplanted s.c. into 5 BALB/c nude mice, respectively. Four weeks later, the tumors were dissected and their weight was determined. Left panel, a picture of mice with tumors of the indicated cell line. Right panel, weights of tumors. The average values of the tumors from 5 mice are indicated by red horizontal bars. (C) PS-exposure in the tumors developed in nude mice. Annexin V-staining profile of the Thy1.2⁺ tumor cells of the indicated cell line is shown. The number indicates the percentage of Annexin V-positive cells.

A**mouse TMEM16F**

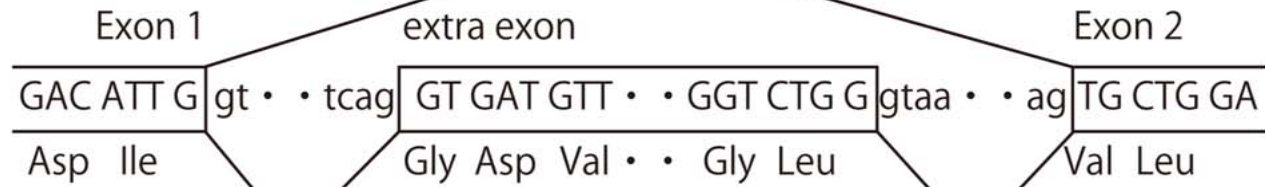
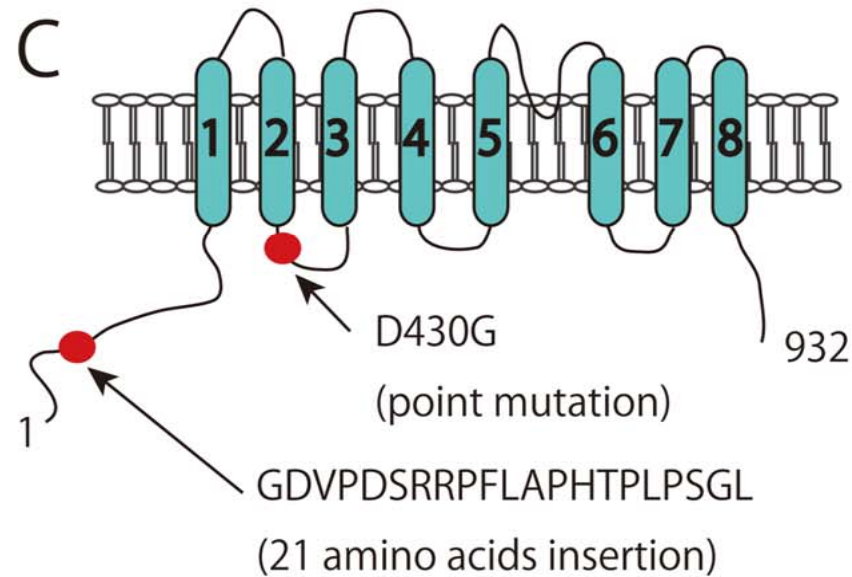
Wild-type



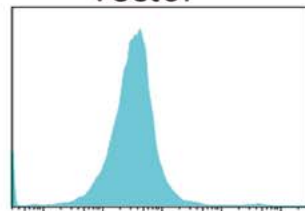
D409G



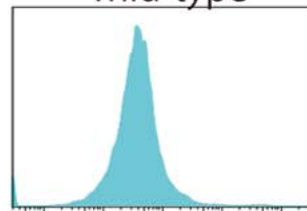
D430G-L

**B****C****D****Ba/F3**

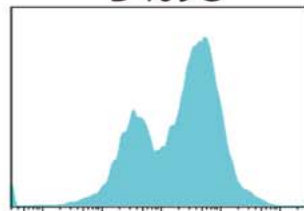
vector



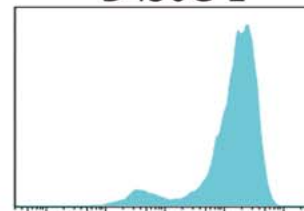
wild-type



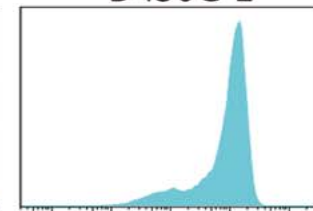
D409G



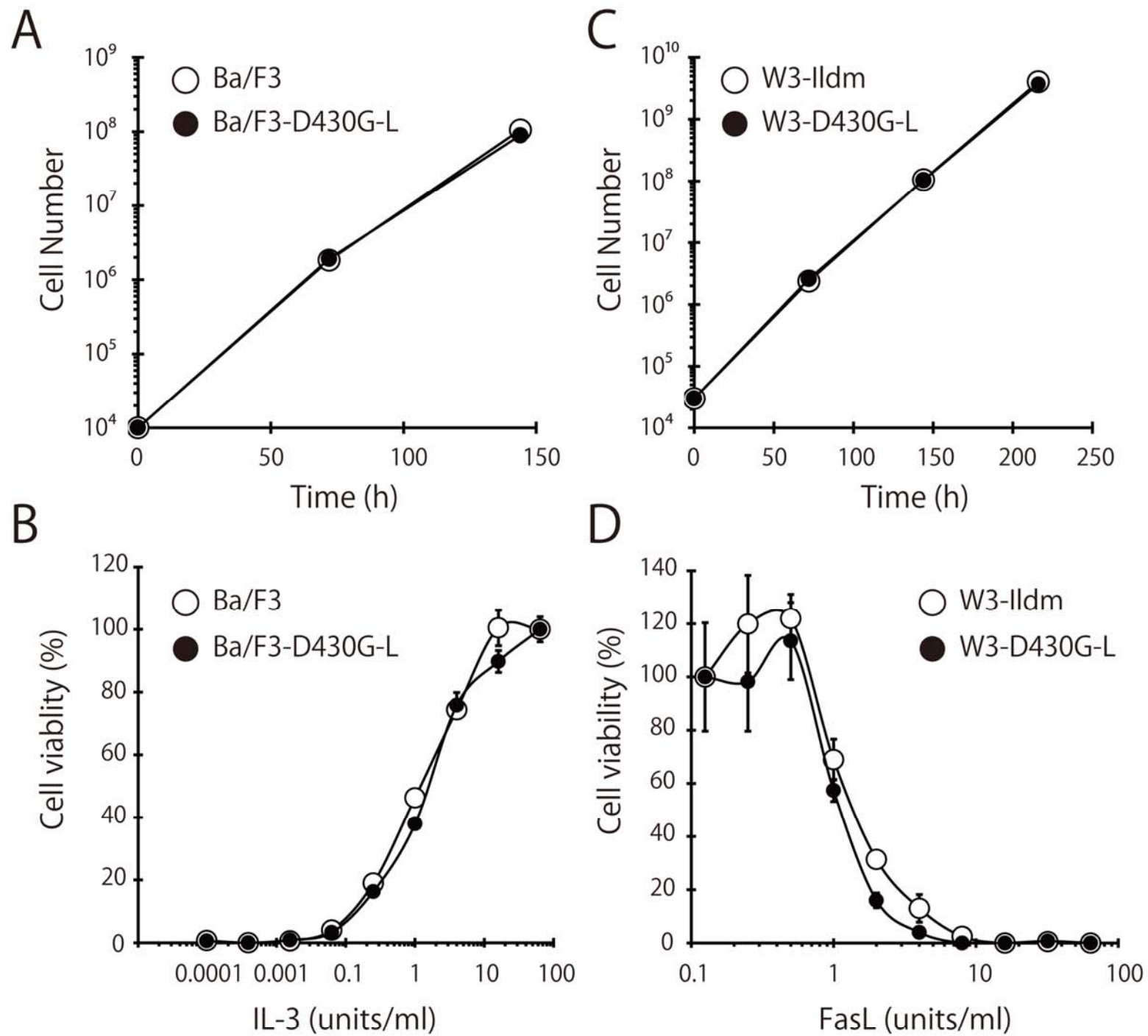
D430G-L

**W3-Ildm**

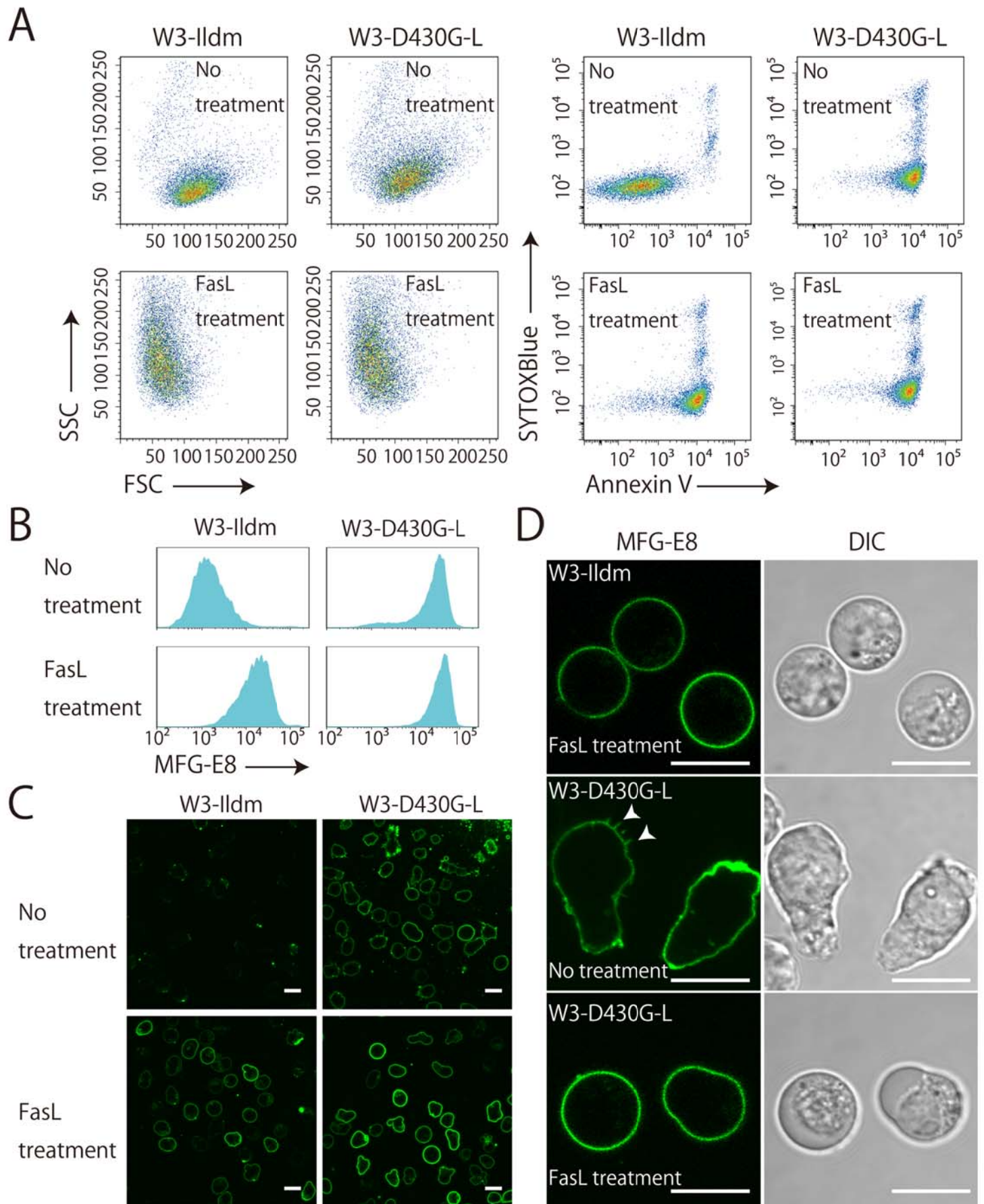
D430G-L



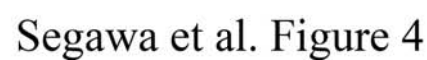
Annexin V →



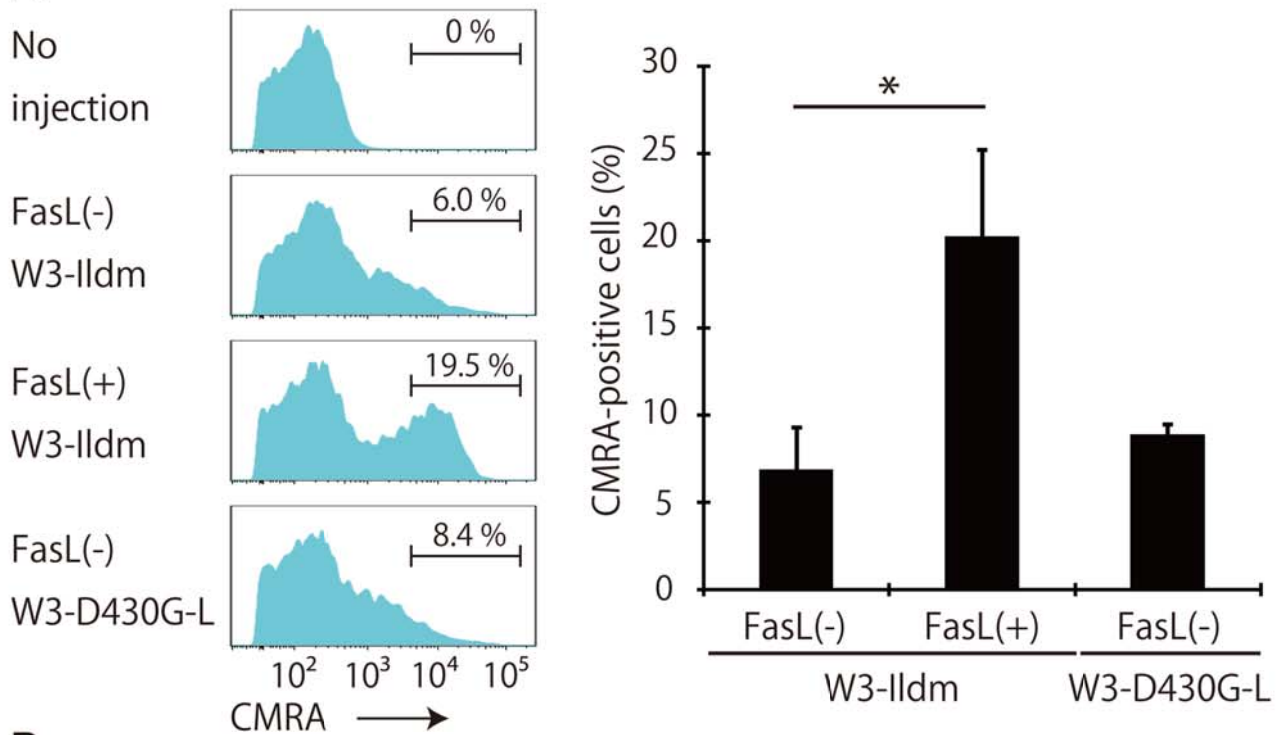
Segawa et al. Figure 2



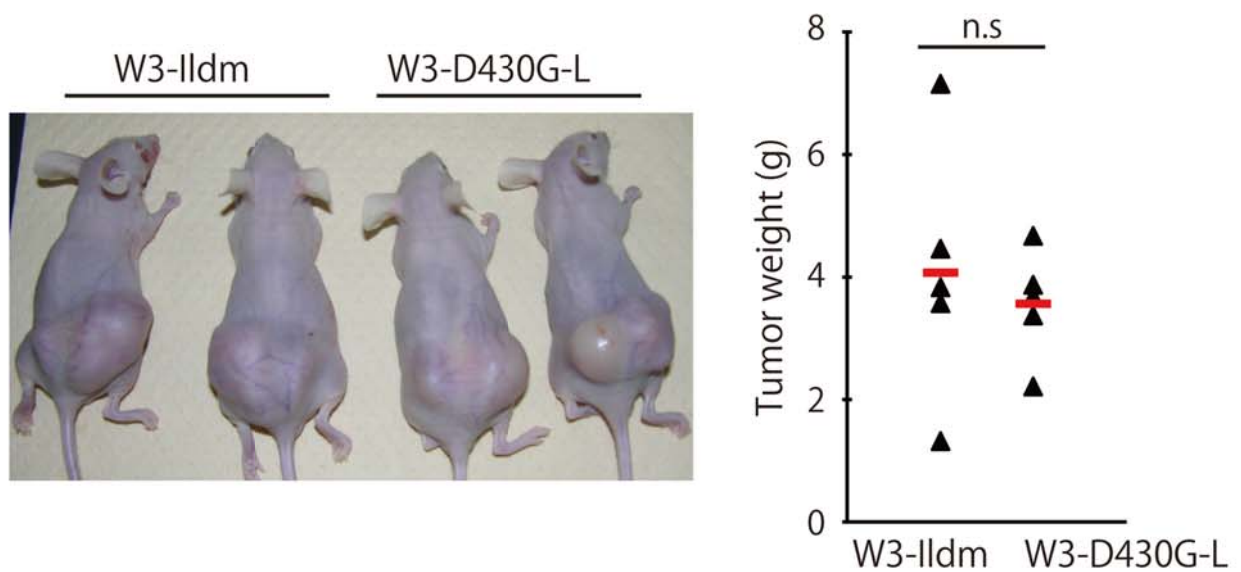
Segawa et al. Figure 3



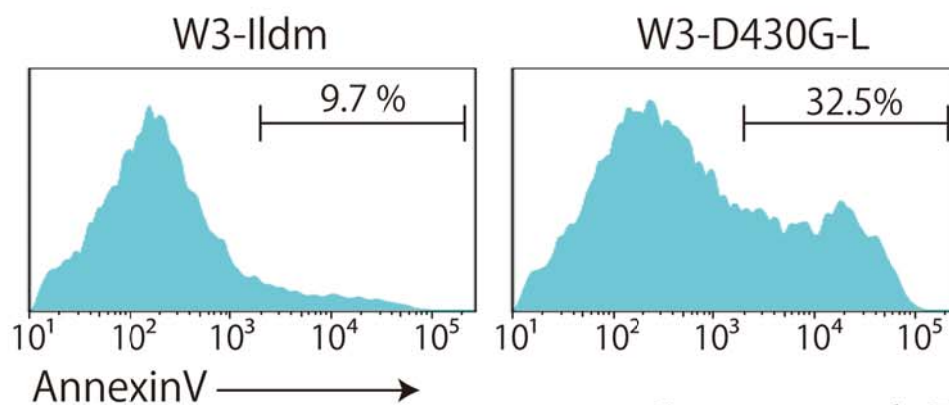
A



B



C



Segawa et al. Figure 5